J Biomol NMR (2013) 55:231–237
DOI 10.1007/s10858-013-9704-3

ARTICLE

# Improving the chemical shift dispersion of multidimensional NMR spectra of intrinsically disordered proteins

**Wolfgang Bermel · Marta Bruix · Isabella C. Felli · Vasantha Kumar M. V. · Roberta Pierattelli · Soraya Serrano**

Received: 2 November 2012 / Accepted: 2 January 2013 / Published online: 12 January 2013


**Abstract** Intrinsically disordered proteins (IDPs) have recently attracted the attention of the scientific community challenging the well accepted structure–function paradigm. In the characterization of the dynamic features of proteins nuclear magnetic resonance spectroscopy (NMR) is a strategic tool of investigation. However the peculiar properties of IDPs, with the lack of a unique 3D structure and their high flexibility, have a strong impact on NMR observables (low chemical shift dispersion, efficient solvent exchange broadening) and thus on the quality of NMR spectra. Key aspects to be considered in the design of new NMR experiments optimized for the study of IDPs are discussed. A new experiment, based on direct detection of $^{13}C^{\alpha}$, is proposed.

**Keywords** Intrinsically disordered proteins · IDP · NMR · Chemical shift · $^{13}C$ NMR · $^{13}C$ direct detection · Secondary structure

W. Bermel
Bruker BioSpin GmbH, 76287 Rheinstetten, Germany

M. Bruix · S. Serrano
Instituto de Quimica Fisica ''Rocasolano'', Consejo Superior de Investigaciones Cientificas, Serrano 119, 28006 Madrid, Spain

I. C. Felli (✉) · R. Pierattelli (✉)
Department of Chemistry "Ugo Shiff", University of Florence, Via della Lastruccia 13, Sesto Fiorentino, 50019 Florence, Italy
e-mail: felli@cerm.unifi.it

R. Pierattelli
e-mail: pierattelli@cerm.unifi.it

I. C. Felli · V. Kumar M. V. · R. Pierattelli
Magnetic Resonance Center, University of Florence, via L. Sacconi 6, Sesto Fiorentino, 50019 Florence, Italy

The lack of a unique protein 3D structure and the high extent of flexibility have recently been shown to provide functional advantages in a variety of biologically relevant situations challenging structural biology and demanding an expansion of the structure–function paradigm into an additional dimension of disorder to be able to describe also intrinsically disordered proteins (IDPs) (Romero et al. 1998; Garner et al. 1998; Wright and Dyson 1999; Tompa 2002, 2009, 2012; Dyson and Wright 2005; Sickmeier et al. 2007; Dunker et al. 2008). In this context NMR is a strategic tool of investigation (Dyson and Wright 2004; Mittag and Forman-Kay 2007; Eliezer 2009; Felli and Pierattelli 2012a, b; Kjaergaard and Poulsen 2012; Felli et al. 2012). However the NMR experiments should be tailored to the general properties of IDPs. Indeed the high extent of flexibility typical of disordered proteins averages out contributions to chemical shifts that otherwise would arise from the presence of well-defined secondary and tertiary structures, causing extensive resonance overlap. The other important characteristic of IDPs consists in the largely solvent-exposed backbone nuclei that cause an increase in the exchange rates of amide protons with the solvent. This may cause broadening beyond detection of amide proton resonances, in particular close to physiological conditions (neutral pH, high temperature). For these reasons heteronuclei ($^{13}C$, $^{15}N$) have always played a major role in the study of unfolded protein states (Schwalbe et al. 1997; Hennig et al. 1999; Dyson and Wright 2001, 2004; Mittag and Forman-Kay 2007). More recently, thanks to the tremendous improvements in instrumental sensitivity, a suite of exclusively heteronuclear NMR experiments based on $^{13}C$ direct detection has been developed to exploit at best the properties of heteronuclei (Bermel et al. 2006a, 2009a, b; Novacek et al. 2011, 2012; Takeuchi et al. 2010a, b; Eletsky et al. 2003; Vögeli et al. 2004, 2005; Richter et al. 2010; Serber et al. 2000, 2001). Indeed it is well known from the

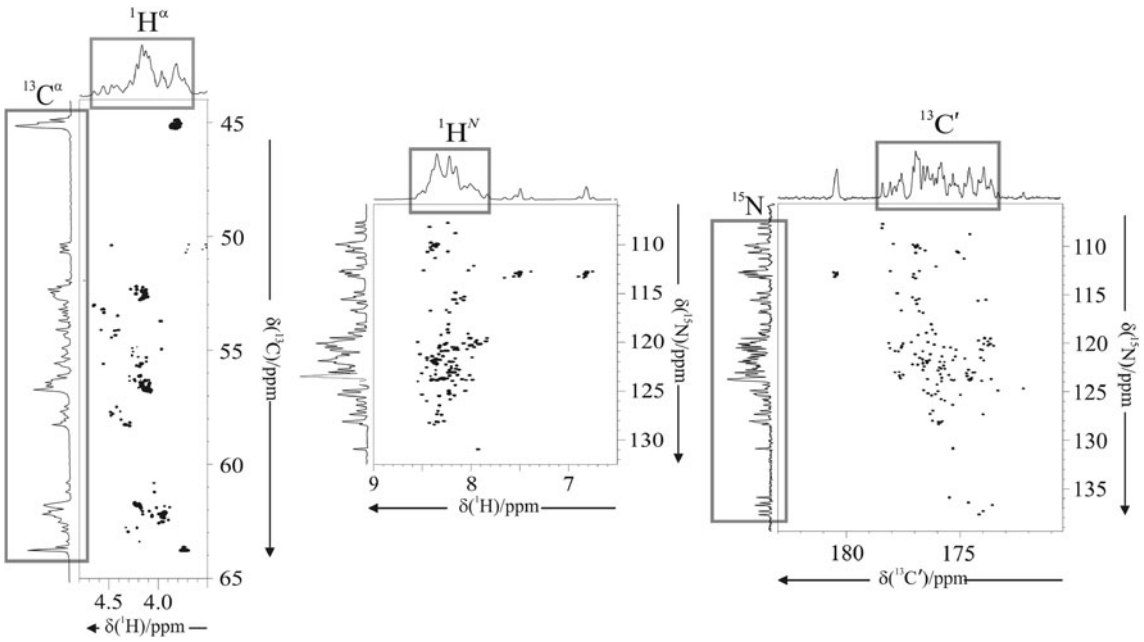


**Fig. 1** 16.4 T $^{1}$H–$^{13}$C HSQC, $^{1}$H–$^{15}$N HSQC and $^{13}$C–$^{15}$N CON spectra acquired on $^{13}$C, $^{15}$N human α-synuclein. The extent of $^{1}H^{\alpha}$, $^{1}H^{N}$, $^{13}C^{\alpha}$, $^{13}C'$, $^{15}$N chemical shift dispersion obtained in the 2D spectra can be fully appreciated in the projections, where the signals belonging to the backbone nuclei are highlighted by *squared boxes*. To enable meaningful comparison of the frequency distribution of resonances, scales were adjusted to be comparable in Hz (obtain the same Hz/cm ratios)

first pages of NMR textbooks that the chemical shift dispersion does increase when going from protons to heteronuclei ($^{13}$C, $^{15}$N). This general feature also holds in the absence of a unique 3D structure such as for IDPs as shown in Fig. 1, which reports the chemical shift ranges observed for different backbone nuclei in human α-synuclein, a paradigmatic, well studied IDP. The $^{1}$H detected 2D experiments ($^{1}$H–$^{13}$C as well as $^{1}$H–$^{15}$N 2D HSQC spectra) clearly show an increase in the chemical shift dispersion passing from $^{1}$H to the directly bound heteronucleus, both for $^{13}C^{\alpha}$ as well as for $^{15}$N, confirming the importance of exploiting heteronuclei to study IDPs. The dispersion of the observed cross peaks also improves going from the $^{1}$H–$^{13}$C to the $^{1}$H–$^{15}$N 2D spectrum. Indeed the latter is one of the most widely used experiments for the characterization of IDPs. Therefore, in addition to the 2D $^{1}$H–$^{15}$N HSQC spectrum (Fig. 1), correlating $^{15}$N to the attached $^{1}$H, one can also exploit the correlation of $^{15}$N with the attached carbonyl carbon ($^{13}C'$) through the 2D CON spectrum (Bermel et al. 2006a), also reported in Fig. 1 for human α-synuclein. The cross peaks in the 2D CON spectrum are well dispersed also for this highly disordered protein of 140 aminoacids, and signals deriving from proline residues are clearly identifiable due to the peculiar $^{15}$N chemical shift of the imino nitrogen, in principle providing a richer source of information compared to that available through 2D $^{1}$H–$^{15}$N correlation spectra. In fact NMR experiments based on direct $^{13}$C carbonyl detection have been used for the characterization of several IDPs and the number of novel applications is continuously increasing (Bermel et al. 2006a, 2012a; Pérez et al. 2009; Hsu et al. 2009; O'Hare et al. 2009; Motackova et al. 2010; Bertini et al. 2011; Novacek et al. 2012).

The chemical shift dispersion of carbonyl carbons, as also evident by comparing it with that observed for $C^{\alpha}$s in human α-synuclein, is one of the smallest ones observed for different types of homologous $^{13}$C spins in proteins. So it might seem surprising that the 2D CON spectra are characterized by such a nice dispersion of the observed cross peaks. However, it should be noted that the correlations observed in CON spectra involve nuclei belonging to *sequential* aminoacids, an aspect that has a significant impact on the dispersion of the correlations observed in NMR spectra of IDPs. As noted before, in the absence of a well-defined protein 3D structure the NMR chemical shifts of the aminoacid nuclei tend to cluster around the values predicted for each aminoacid-type, with small additional contributions arising from the nature of the previous and following aminoacids in the primary sequence (Schwarzinger et al. 2001; Tamiola et al. 2010; Kjaergaard and Poulsen 2011, 2012). The effect is particularly striking when observing the 2D $^{1}$H–$^{13}$C correlation map of human α-synuclein, part of which is shown in Fig. 1 ($^{1}H^{\alpha}$–$^{13}C^{\alpha}$ portion). Despite the large dispersion of $^{13}$C shifts, and the very high resolution used to acquire the spectrum, the number of cross peaks that can be resolved is very small, much less than expected for this 140 aminoacids protein, essentially due to clustering of correlations that derive from the same type of aminoacids in specific spectral regions.

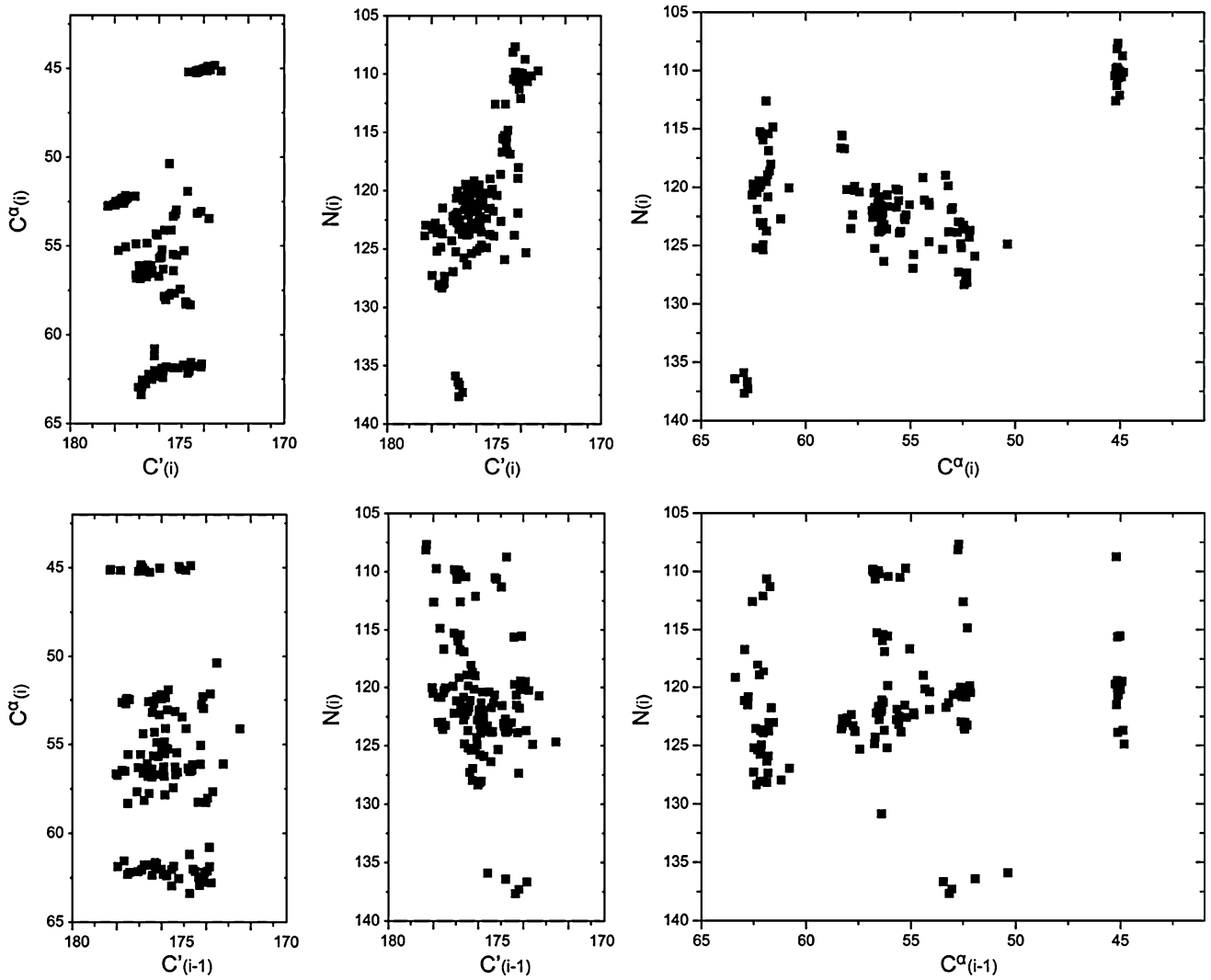


**Fig. 2** Plots of the correlation between C′-C$^{\alpha}$, C′-N and C$^{\alpha}$-N generated using as input experimental chemical shifts measured for human α-synuclein (BMRB 6968)(Bermel et al. 2006a). Axes scales are in ppm. The comparison between the *top panels* (intra-residue correlations) and the *bottom panels* (inter-residue correlations) clearly demonstrates that the inter-residue nature of the correlations contributes dramatically to cross peak dispersion in IDPs. For folded proteins this is less evident as their nuclei experience much larger contributions to chemical shifts arising from the presence of secondary and tertiary structures

This shows that, while on one hand these characteristic intra-residue $^{1}$H–$^{13}$C cross peaks provide a clear fingerprint of different aminoacid-types, they do not help in resolving spectral overlaps for aminoacids of the same kind.

These general trends for chemical shifts observed in IDPs are well known and are widely used to predict random coil chemical shifts for the nuclei of a protein on the basis of its primary sequence using typical shifts for each aminoacid as well as correction factors derived from the presence of specific aminoacids in positions $i_{(\pm 1)}$ and $i_{(\pm 2)}$ (Wishart et al. 1995; Schwarzinger et al. 2001; De Simone et al. 2009; Kjaergaard and Poulsen 2011). These calculated chemical shifts are generally used as a reference to compare them with experimentally observed chemical shifts in order to identify regions characterized by secondary structural propensities, if any, in IDPs (Marsh et al. 2006, 2010; Mukrasch et al. 2009; Bertini et al. 2011; Tamiola and Mulder 2012). These predictors as well as the body of data acquired on naturally or chemically unstructured proteins do confirm that the main contributions to chemical shifts arise from the nature of the aminoacid, with the direct consequence that intra-residue correlations are poorly resolved.

It is thus instructive to predict the dispersion of cross peaks in 2D maps correlating backbone heteronuclei either coming from the same aminoacid or from neighboring aminoacids in the primary sequence as shown in Fig. 2, built taking as an example experimental chemical shifts of human α-synuclein (BMRB 6968) (Bermel et al. 2006a). The figure, which reports in the top panels the intra-residue

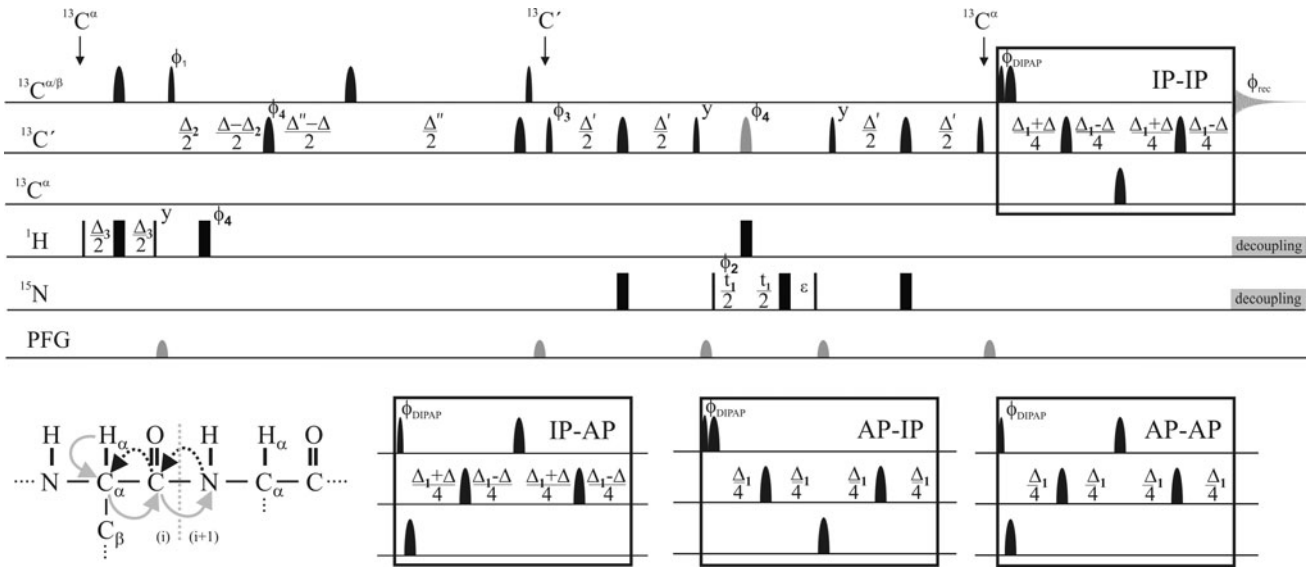


**Fig. 3** 2D inter-CAN NMR experiment. The delays used $\Delta_1 =$ 14.4 ms, $\Delta = 9$ ms, $\Delta_2 = 2.2$ ms, $\Delta_3 = 3.6$ ms, $\Delta' = 24.8$ ms and $\Delta'' = 26.6$ ms $\varepsilon =$ $t_1(0) +$ pC180 which is shown as grey pulse in the middle of $^{15}$N chemical shift evolution time. The phase cycle is: $\phi_1 = 4(x), 4(-x)$, $\phi_2 = 2(x), 2(-x)$, $\phi_3 = x, -x$, $\phi_4 = 8(x), 8(-x)$, $\phi_{DIPAP}$ (IPIP) $= x$; $\phi_{DIPAP}$ (APIP) $= -y$; $\phi_{DIPAP}$ (IPAP) $= -y$; $\phi_{DIPAP}$ (APAP) $= -x$; $\phi_{rec} = x, 2(-x), x, -x, 2(x), -x$. Quadrature detection in F1 dimension is obtained by incrementing $\phi_2$ in a States-TPPI manner. The coherence transfer pathway exploits the one-bond scalar couplings $^1J_{H\alpha C\alpha}$, $^1J_{C\alpha C'}$, $^1J_{C'N}$, as schematically illustrated. The pulse sequence starts with $^1$H polarization ($^1$H-start) that, after the first $^1$H 90° pulse, is transferred to $^{13}C^{\alpha}$ through the evolution of the $^1J_{H\alpha C\alpha}$, then to $^{13}C'$ (through the evolution of the $^1J_{C\alpha C'}$), and finally to $^{15}$N (through the evolution of the $^1J_{C'N}$). Frequency labeling of $^{15}$N is then achieved to create the indirect $^{15}$N dimension, followed by back transfers to $^{13}C'$ and then to $^{13}C^{\alpha}$ (through the evolution of the $^1J_{C'N}$ and $^1J_{C\alpha C'}$ respectively) prior to direct detection of $^{13}C^{\alpha}$. The four different variants to implement $^{13}C^{\alpha}$ homonuclear decoupling differ by the position of the band-selective $^{13}$C 180° pulses on $^{13}C'$, $^{13}C^{\alpha}$, $^{13}C^{\alpha/\beta}$, indicated using the first three lines in the pulse scheme

correlations and in the bottom panels the inter-residue ones for a selected sub-set of backbone heteronuclear spin pairs, clearly shows that the inter-residue nature of correlations provides an important contribution to reducing the potential overlaps in spectra of IDPs. This is likely to be a general feature for IDPs while it is not so important for folded proteins which experience many additional contributions to chemical shift dispersion. This observation explains why the highly sensitive CACO spectrum suffers from strong overlap when acquired on IDPs, essentially because of the intra-residue nature of the correlations it gives, while the CON spectrum, which correlates two nuclear spins involved in the peptide bond, is instead characterized by an improved chemical shift dispersion of the cross peaks.

To exploit this finding we can design inter-residue versions of the 2D experiments involving backbone heteronuclei such as the inter-CACO and inter-CAN, where the $C^{\alpha}$–N is a very useful correlation for assignment (Takeuchi et al. 2008, 2010a) but again affected by poor chemical shift dispersion in the intra-residue mode. The inter-residue correlations between $C^{\alpha}$ and $C'$ spins can easily be detected by acquiring the 2D CACO plane of CANCO experiments (Bertini et al. 2004; Bermel et al. 2005b), based on carbonyl direct detection. Concerning the inter-CAN experiment, this would of course provide a very interesting complementary experiment respect to the ones that are already available thanks to the wide chemical shift range of both nuclear spins as well as to its inter-residue nature. However the experiment is based on direct detection of $C^{\alpha}$ spins, so that, unless specific isotopic labeling strategies are employed (Takeuchi et al. 2010a, b), it is very important to take care of homonuclear $^{13}$C decoupling to achieve a good resolution, in particular for IDPs. Otherwise all the advantage of going to heteronuclear detection would be lost by quadrupling/doubling the number of expected signals for $C^{\alpha}$ spins that do couple with a $C^{\beta}$ spin (except for glycines), in addition to carbonyls. To this end, several solutions have recently been proposed in the literature for the study of large proteins (Bermel et al. 2005a, 2007). They all rely on acquisition of different independent components of the in-phase (IP) and antiphase (AP) multiplets either by allowing full interconversion between the two (IPAP-type) or only partial ($S^3$E-type), with the latter requiring about half the time for magnetization to be transverse (Bermel et al. 2008). Among the different strategies proposed, we decided to focus on the IPAP-type approach (Duma et al. 2003; Bermel et al. 2005a, 2007) as

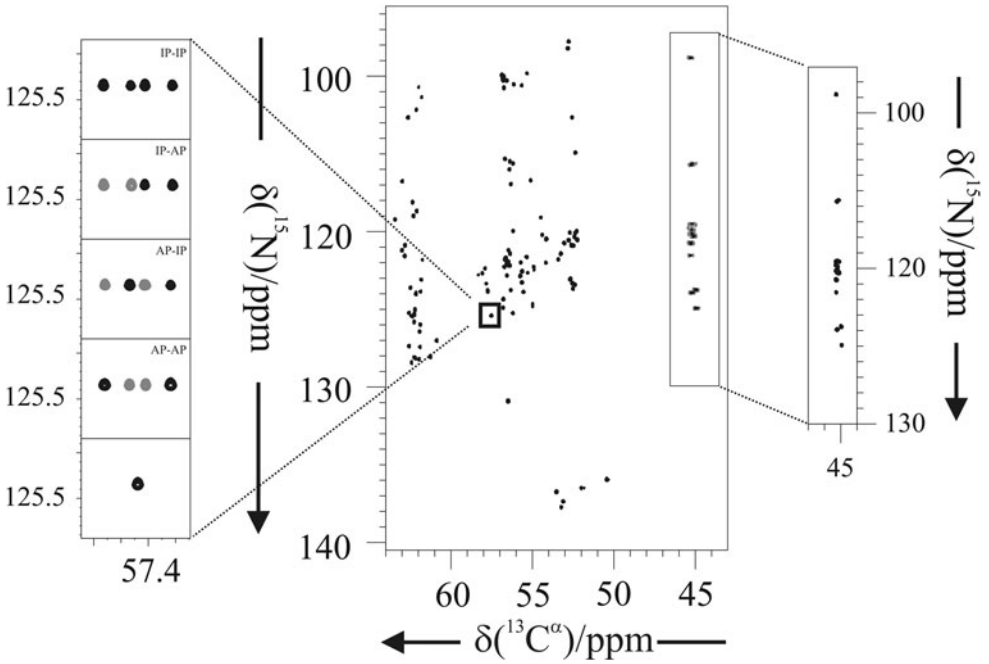


**Fig. 4** 16.4 T inter-CAN spectrum acquired on $^{13}C$, $^{15}N$ human α-synuclein. The portions extracted for an arbitrary peak from the four different sub-spectra of the inter-CAN before combining them to perform homonuclear decoupling and their combination to obtain a singlet are reported on the left. In the insert on the right, the region where glycine residues resonate taken from the spectrum processed omitting the removal of the $J_{C\alpha C\beta}$ coupling is reported (see Experimental part). The inter-CAN experiment was recorded with 16 scans per increment with an inter-scan delay of 1.2 s for a total duration of 14 h. In the obtained 2D spectrum the average distance between two neighbors, which is a well-accepted measure of the dispersion of a set of points in the n-dimensional space (Clark and Evans, 1954), is 0.72 ppm, while it would be only 0.42 ppm in the corresponding CAN experiment

for most of the IDPs, that are amenable to NMR, transverse relaxation rates are compatible with its implementation. The pulse sequence used to acquire the inter-CAN experiment on human α-synuclein is reported in Fig. 3. It starts with $^{1}H^{\alpha}$ polarization, exploits coherence transfer steps mediated by one-bond scalar couplings ($^{1}J_{H\alpha C\alpha}$, $^{1}J_{C\alpha C'}$, $^{1}J_{C'N}$) and the IPAP-type approach to achieve homonuclear $^{13}C^{\alpha}$ decoupling (DIPAP). The four different multiplet components that are acquired to perform homonuclear $^{13}C^{\alpha}$ decoupling are shown as an example in Fig. 4, together with the final 2D inter-CAN spectrum that can be obtained. For glycine aminoacids, which lack one of the two large carbon–carbon homonuclear couplings, it is sufficient to process the spectra in a different way (Fig. 4, right insert). As expected, the 2D spectrum is characterized by a good dispersion of the cross peaks and can thus provide a valuable tool to investigate IDPs, in particular in cases in which amide protons are extensively broadened by solvent exchange processes. On the other hand, increase in transverse relaxation rates of other nature impact on the sensitivity of the experiment.

Concluding we have shown that one important aspect for the design of experiments optimized for the study of IDPs, in addition to the large heteronuclear chemical shift dispersion, is the ability to exploit as much as possible correlations between nuclei belonging to different aminoacids to improve the chemical shift dispersion and thus reduce signal overlap. This can be used as a general concept to implement new multidimensional experiments. The 2D inter-CAN experiment, based on $C^{\alpha}$ direct detection, is proposed here as an extra tool, to be used in conjunction with the 2D CON, to follow chemical shifts of IDPs also in cases in which amide protons may be broadened beyond detection.

## Experimental part

A sample of 1.0 mM uniformly $^{13}C$, $^{15}N$ labeled human α-synuclein in 20 mM phosphate buffer at pH 6.5 was prepared as previously described (Bermel et al. 2012b). EDTA and NaCl were added to reach the final concentration of 0.5 mM and 200 mM, respectively, and 10 % $D_2O$ was added for the lock. All NMR experiments were performed at 285.5 K, 16.4 T on a Bruker Avance spectrometer operating at 700.06 MHz $^{1}H$ and 176.03 MHz $^{13}C$ frequencies, equipped with a $^{13}C$ cryogenically cooled probehead optimized for $^{13}C$-direct detection. For $^{13}C$ band-

selective $\pi/2$ and $\pi$ flip angle pulses Q5 (or time reversed Q5) and Q3 shapes (Emsley and Bodenhausen 1992) of durations of 300 and 220 μs, respectively, were used, except for the $\pi$ pulses that should be band-selective on the $C^{\alpha}$ region (Q3, 860 μs) and for the adiabatic $\pi$ pulse to invert both $C'$ and $C^{\alpha}$ (smoothed Chirp 500 μs, 25 % smoothing, 80 kHz sweep, 11.3 kHz RF field strength (Boehlen and Bodenhausen 1993)). The $^{13}C$ band selective pulses on $C^{ali}$, $C^{\alpha}$, and $C'$ were given at the center of each region and the adiabatic pulse was adjusted to cover the entire $^{13}C$ region. Decoupling of $^{1}H$ and $^{15}N$ was achieved with waltz16 (Shaka et al. 1983) (1.7 kHz) and garp4 (Shaka et al. 1985) (1.0 kHz) sequences, respectively. All gradients employed had 1 ms of duration. In experiments that employ the DIPAP block (Bermel et al. 2005a, 2006b), for each time increment in the indirect dimension, four FIDs were separately stored, and the resulting sub-matrices were added and subtracted in pairs to separate the four multiplet components, then shifted by ($\pm J_{C'C\alpha}/2$) and ($\pm J_{C\alpha C\beta}/2$ Hz) and summed again to obtain a singlet. The spin-state-selection approach can also be implemented to achieve $^{15}N$ decoupling in order to be able to extend the acquisition of the FID without limitations imposed by $^{15}N$ decoupling (Bermel et al. 2009a). The other experimental parameters used to acquire spectra shown are described in the figure captions. Spectra were acquired and processed using the standard Bruker TopSpin 1.3 software.

**Acknowledgments** This work has been supported in part by the Joint Research Activity and Access to Research Infrastructures (Bio–NMR, contract 261863) and by the Marie Curie ITN programs (ID-PbyNMR, contract 264257) in the EC 7th Framework. S·S. acknowledges financial support for a short stay fellowship associated to Project CTQ2008–0080 from the Spanish Ministerio de Economía y Competitividad.

## References

Bermel W, Bertini I, Duma L, Emsley L, Felli IC, Pierattelli R, Vasos PR (2005a) Complete assignment of heteronuclear protein resonances by protonless NMR spectroscopy. Angew Chem Int Ed 44:3089–3092

Bermel W, Bertini I, Felli IC, Pierattelli R, Vasos PR (2005b) A selective experiment for the sequential protein backbone assignment from 3D heteronuclear spectra. J Magn Reson 172:324–328

Bermel W, Bertini I, Felli IC, Lee Y-M, Luchinat C, Pierattelli R (2006a) Protonless NMR experiments for sequence-specific assignment of backbone nuclei in unfolded proteins. J Am Chem Soc 128:3918–3919

Bermel W, Bertini I, Felli IC, Piccioli M, Pierattelli R (2006b) $^{13}C$-detected *protonless* NMR spectroscopy of proteins in solution. Progr NMR Spectrosc 48:25–45

Bermel W, Felli IC, Matzapetakis M, Pierattelli R, Theil EC, Turano P (2007) A method for $C^{\alpha}$ direct-detection in protonless NMR. J Magn Reson 188:301–310

Bermel W, Felli IC, Kümmerle R, Pierattelli R (2008) $^{13}C$ direct-detection biomolecular NMR. Concepts Magn Reson 32A:183–200

Bermel W, Bertini I, Csizmok V, Felli IC, Pierattelli R, Tompa P (2009a) H-start for exclusively heteronuclear NMR spectroscopy: the case of intrinsically disordered proteins. J Magn Reson 198:275–281

Bermel W, Bertini I, Felli IC, Pierattelli R (2009b) Speeding up $^{13}C$ direct detection NMR experiments. J Am Chem Soc 131: 15339–15345

Bermel W, Bertini I, Chill JH, Felli IC, Kumar VMV, Haba N, Pierattelli R (2012a) Aminoacid-types selective $^{13}C$ direct-detected exclusively heteronuclear experiments to study intrinsically disordered proteins. Chem Bio Chem 13:2425–2432

Bermel W, Bertini I, Gonnelli L, Felli IC, Kozminski W, Piai A, Pierattelli R, Stanek J (2012b) Speeding up sequence specific assignment of IDPs. J Biomol NMR 53:293–301

Bertini I, Duma L, Felli IC, Fey M, Luchinat C, Pierattelli R, Vasos PR (2004) A heteronuclear direct detection NMR experiment for protein backbone assignment. Angew Chem Int Ed 43:2257–2259

Bertini I, Felli IC, Gonnelli L, Kumar VMV, Pierattelli R (2011) High-resolution characterization of intrinsic disorder in proteins: expanding the suite of $^{13}C$ detected NMR experiments to determine key observables. ChemBioChem 12:2347–2352

Boehlen J-M, Bodenhausen G (1993) Experimental aspects of chirp NMR spectroscopy. J Magn Reson Ser A 102:293–301

Clark PJ, Evans FC (1954) Distance to nearest neighbor as a measure of spatial relationships in populations. Ecology 35:445–453

De Simone A, Cavalli A, Hsu ST, Vranken W, Vendruscolo M (2009) Accurate random coil chemical shifts from an analysis of loop regions in native states of loop regions in native states of proteins. J Am Chem Soc 131:16332–16333

Duma L, Hediger S, Lesage A, Emsley L (2003) Spin-state selection in solid-state NMR. J Magn Reson 164:187–195

Dunker AK, Silman I, Uversky VN, Sussman JL (2008) Function and structure of inherently disordered proteins. Curr Opin Struct Biol 18:756–764

Dyson HJ, Wright PE (2001) Nuclear magnetic resonance methods for the elucidation of structure and dynamics in disordered states. Methods Enzymol 339:258–271

Dyson HJ, Wright PE (2004) Unfolded proteins and protein folding studied by NMR. Chem Rev 104:3607–3622

Dyson HJ, Wright PE (2005) Intrinsically unstructured proteins and their functions. Nat Rev Mol Cell Biol 6:197–208

Eletsky A, Moreira O, Kovacs H, Pervushin K (2003) A novel strategy for the assignment of side-chain resonances in completely deuterated large proteins using $^{13}C$ spectroscopy. J Biomol NMR 26:167–179

Eliezer D (2009) Biophysical characterization of intrinsically disordered proteins. Curr Opin Struct Biol 19:23–30

Emsley L, Bodenhausen G (1992) Optimization of shaped selective pulses for NMR using a quaternion description of their overall propagators. J Magn Reson 97:135–148

Felli IC, Pierattelli R (2012a) $^{13}C$ direct detection NMR. In: McGreevy KS, Parigi G, Bertini I (eds) NMR of biomolecules. Wiley, Newyork, pp 433–442

Felli IC, Pierattelli R (2012b) Recent progress in NMR spectroscopy: toward the study of intrinsically disordered proteins of increasing size and complexity. IUBMB Life 64:473–481

Felli IC, Pierattelli R and Tompa P (2012) Intrinsically disordered proteins. In: Bertini I, McGreevy KS, Parigi G (eds) Wiley, Newyork, 137-152

Garner E, Cannon P, Romero P, Obradovic Z, Dunker AK (1998) Predicting disordered regions from aminoacid sequence: common themes despite differing structural characterization. Genome Inform 9:201–213

Hennig M, Bermel W, Spencer A, Dobson CM, Smith LJ, Schwalbe H (1999) Side-chain conformations in an unfolded protein: $\chi_1$

distributions in denaturated hen lysozyme determined by heteronuclear $^{13}C$, $^{15}N$ NMR spectroscopy. J Mol Biol 288:705–723

Hsu ST, Bertoncini CW, Dobson CM (2009) Use of protonless NMR spectroscopy to alleviate the loss of information resulting from exchange to broadening. J Am Chem Soc 131:7222–7223

Kjaergaard M, Poulsen FM (2011) Sequence correction of random coil chemical shifts: correlation between neighbor correction factors and changes in the Ramachandran distribution. J Biomol NMR 50:157–165

Kjaergaard M, Poulsen FM (2012) Disordered proteins studied by chemical shifts. Prog NMR Spectrosc 60:42–51

Marsh JA, Singh VK, Jia Z, Forman-Kay JD (2006) Sensitivity of secondary structural propensities to sequence differences between α-and γ-synuclein: implications for fibrillation. Protein Sci 15:2795–2804

Marsh JA, Dancheck B, Ragusa MJ, Allaire M, Forman-Kay JD, Peti W (2010) Structural diversity in free and bound states of intrinsically disordered protein phosphatase 1 regulators. Structure18: 1094–1103

Mittag T, Forman-Kay J (2007) Atomic-level characterization of disordered protein ensembles. Curr Opin Struct Biol 17:3–14

Motackova V, Novacek J, Zawadzka-Kazimierczuk A, Kazimierczuk K, Zidek L, Sanderová H, Krasny L, Kozminski W, Sklenar V (2010) Strategy for complete NMR assignment of disordered proteins with highly repetitive sequences based on resolution-enhanced 5D experiments. J Biomol NMR 48:169–177

Mukrasch MD, Bibow S, Korukottu J, Jeganathan S, Biernat J, Griesinger C, Mendelkow E, Zweckstetter M (2009) Structural polimorphism of 441-residue tau at single residue resolution. PLoS Biol 7:e34

Novacek J, Zawadzka-Kazimierczuk A, Papoušková V, Zidek L, Sanderová H, Krasny L, Kozminski W, Sklenar V (2011) 5D $^{13}C$-detected experiments for backbone assignment of unstructured proteins with a very low signal dispersion. J Biomol NMR 50:1–11

Novacek J, Haba NY, Chill JH, Zidek L, Sklenar V (2012) 4D Non-uniformly sampled HCBCACON and (1) J[NC (α)]-selective HCBCANCO experiments for the sequential assignment and chemical shift analysis of intrinsically disordered proteins. J Biomol NMR 53:139–148

O'Hare B, Benesi AJ, Showalter SA (2009) Incorporating $^{1}H$ chemical shift determination into $^{13}C$-direct detected spectroscopy of intrinsically disordered proteins in solution. J Magn Reson 200:354–358

Pérez Y, Gairi M, Pons M, Bernadó P (2009) Structural characterization of the natively unfolded N-terminal domain of human c-Src kinase: insights into the role of phosphorylation of the unique domain. J Mol Biol 391:136–148

Richter C, Kovacs H, Buck J, Wacker A, Fuertig B, Bermel W, Schwalbe H (2010) $^{13}C$-direct detected NMR experiments for the sequential J-based resonance assignment of RNA oligonucleotides. J Biomol NMR 47:259–269

Romero P, Obradovic Z, Kissinger CR, Villafranca JE, Garner E, Guillot S, Dunker AK (1998) Thousands of proteins likely to have long disordered regions. Pac Symp Biocomputing 3:437–448

Schwalbe H, Fiebig KM, Buck M, Jones JA, Grimshaw SB, Spencer A, Glaser SJ, Smith LJ, Dobson CM (1997) Structural and dynamical properties of a denatured protein. Heteronuclear 3D NMR experiments and theoretical simulations of lysozyme in 8 M urea. Biochem 36:8977–8991

Schwarzinger S, Kroon GJA, Foss TR, Chung J, Wright PE, Dyson HJ (2001) Sequence-dependent correction of random coil NMR chemical shifts. J Am Chem Soc 123:2970–2978

Serber Z, Richter C, Moskau D, Boehlen J-M, Gerfin T, Marek D, Haeberli M, Baselgia L, Laukien F, Stern AS, Hoch JC, Dötsch V (2000) New carbon-detected protein NMR experiments using cryoprobes. J Am Chem Soc 122:3554–3555

Serber Z, Richter C, Dötsch V (2001) Carbon-detected NMR experiments to investigate structure and dynamics of biological macromolecules. ChemBioChem 2:247–251

Shaka AJ, Keeler J, Freeman R (1983) Evaluation of a new broadband decoupling sequence: WALTZ-16. J Magn Reson 53:313–340

Shaka AJ, Barker PB, Freeman R (1985) Computer-optimized decoupling scheme for wideband applications and low-level operation. J Magn Reson 64:547–552

Sickmeier M, Hamilton JA, LeGall T, Vacic V, Cortese MS, Tantos A, Szabo B, Tompa P, Chen J, Uversky VN, Obradovic Z, Dunker AK (2007) DisProt: the database of disordered proteins. Nucleic Acids Res 35:D786–D793

Takeuchi K, Sun ZN, Wagner G (2008) Alternate $^{13}C$–$^{12}C$ labeling for complete main-chain resonance assignments using $C^{\alpha}$ direct-detection with applicability toward fast relaxing protein systems. J Am Chem Soc 130:17210–17211

Takeuchi K, Frueh DP, Hyberts SG, Sun ZYJ, Wagner G (2010a) High-resolution 3D CANCA NMR experiments for complete main chain assignments using $C^{\alpha}$ direct detection. J Am Chem Soc 132:2945–2951

Takeuchi K, Frueh DP, Sun ZYJ, Hiller S, Wagner G (2010b) CACA-TOCSY with alternate $^{13}C$–$^{12}C$ labeling: a $^{13}C^{\alpha}$ direct detection experiment for main chain resonance assignment, dihedral angle information and aminoacid type identification. J Biomol NMR 47:55–63

Tamiola K, Mulder FA (2012) Using NMR chemical shifts to calculate the propensity for structural order and disorder in proteins. Biochem Soc Trans 10:1014–1020

Tamiola K, Acar B, Mulder FAA (2010) Sequence-specific random coil chemical shifts of intrinsically disordered proteins. J Am Chem Soc 132:18000–18003

Tompa P (2002) Intrinsically unstructured proteins. Trends Biochem Sci 27:527–533

Tompa P (2009) Structure and function of intrinsically disordered proteins. Taylor and Francis Group, Boca Raton, FL

Tompa P (2012) Intrinsically disordered proteins: a 10-year recap. Trends Biochem Sci

Vögeli B, Kovacs H, Pervushin K (2004) Measurements of side chain $^{13}C$–$^{13}C$ residual dipolar coupling in uniformly deuterated proteins. J Am Chem Soc 126:2414–2420

Vögeli B, Kovacs H, Pervushin K (2005) Simultaneous $^{1}H$- or $^{2}H$-, $^{15}N$- and multiple-band-selective $^{13}C$-decoupling during acquisition in $^{13}C$-detected experiments with proteins and oligonucleotides. J Biomol NMR 31:1–9

Wishart DS, Bigam CG, Holm A, Hodges RS, Sykes BD (1995) $^{1}H$, $^{13}C$ and $^{15}N$ random coil NMR chemical shifts of the common amino acids. I. Investigations of nearest-neighbor effects. J Biomol NMR 5:67–81

Wright PE, Dyson HJ (1999) Intrinsically unstructured proteins: re-assessing the protein structure-function paradigm. J Mol Biol 293:321–331